Key Engineering Materials
ISSN: 1662-9795, Vol. 926, pp 2031-2039
doi:10.4028/p-0cnty5

Submitted: 2021-12-08
Revised: 2022-01-28
Accepted: 2022-02-03
Online: 2022-07-22

Intelligent Iterative Experimental Design to Achieve Maximum Model Quality for Phase Change of 22MnB5

Thawin Hart-Rawung[1,a*], Johannes Buhl[1,b], Sebastian Härtel[1,c], Markus Bambach[2,d]

[1]Chair of Hybrid Manufacturing, Brandenburg University of Technology, Cottbus - Senftenberg, Konrad - Wachsmann - Allee 17, Cottbus D-03046, Germany

[2]Advanced Manufacturing, Department of Mechanical and Process Engineering, ETH Zurich, Zurich CH-8005, Switzerland

[a]thawihar@b-tu.de, [b]johannes.buhl@b-tu.de, [c]Sebastian.Haertel@b-tu.de, [d]mbambach@ethz.ch

Keywords: Optimal Experimental Design (OED), JMAK, Material modeling, optimization, press hardening.

Abstract. Conducting experiments for material modeling is very costly and time-consuming when many parameters are involved, resulting in a large number of test conditions. Therefore, it is expedient to develop algorithms for the iterative identification of optimal test conditions. This method should allow the model to learn automatically so that only a small number of test conditions are selected at the beginning of the model calibration. In order to decide whether further experiments should be carried out and which test conditions need to be investigated, meta-models are generated, and the expected gain score is calculated. The next sample is selected based on the highest score, and this procedure continues until the material models meet a termination criteria. The result from the study shows that the implemented method uses 12 test conditions to generate a phase transformation model for 22MnB5 steel. The material models fitted with the proposed method provide acceptable predictions when compared with experimental data.

Introduction

The hot stamping process, a combination of forming and heat-treatment, has been used in the automotive industry [1,2]. To design the hot stamping process, simulation has been extensively carried out in many works detailed in refs. [3,4]. This virtual process design based on numerical simulations can help to shorten process development times and to identify problem areas at an early stage, thus enabling cost- and resource-efficient production.

The accuracy of simulation models, however, depends decisively on the quality of the constitutive equations ("material models") used. The majority of material models used in forming technology are phenomenological in nature, i.e. the models are the result of a large number of individual experiments, the results of which have been systematized and described with the aid of parameter-dependent mathematical model equations.

Conventionally, the test conditions are determined before optimization or model fitting. For example, in the hot stamping process, Aziz et al.[5] used a Design of Experiments methods (DOE) with full-factorial test matrix of temperature of cooling water and quenching time to model the hardness properties. Moreover, DOE with full-factorial design was employed by You et al. [6] to model the effect of the process and material variables on the formability of hot stamping process, and by Horn et al. [7] to investigate the influence of the process parameters on the mechanical properties of the local carburization of the hot stamping steel. More information about DOE and its application can be found in Berger et al. [8]. Gunst et al. [9] highlight the fundamental concept, design strategies, and statistical properties of fractional factorial design. An example for a two level half factorial design can be found in [10].

Alternatively, Optimal Experimental Design (OED) approaches as presented in [11,12] can be used to select the best material tests for model identification. This approach has been implemented in many works as following. Lohmar et al. [13] have developed an algorithm to continuously improve

a process model based on production data from a plate mill in order to use the model for the precise prediction of rolling forces. The usage of OED is known in material modeling, where Valadimirov el al. [14] and Bambach et al [15] presented the identification of material models and parameters in plasticity models. In both cases, it is assumed that the best or true constitutive model is not known a priori, but that it must also be determined from experiments. In Bambach et al. [16], an algorithm for the iterative sequential approach of optimal test conditions for warm flow curves is developed, which should allow the model to learn automatically. The strategy achieves the desired accuracy of the material model by utilizing about a half of test matrix representing a full-factorial design. Additionally, Wiebenga el at. [17] used sequential robust optimization to identify optimal process parameters for V-bending process. Here, statistical methods are used to estimate optimal new test conditions and the expected improvement in model quality. The expected improvement is calculated by taking the difference between a functional values obtained from a metamodel with respect to the minimum feasible tested (or calculated) response of the true objective function value.

In the previous paragraph, OED has been implemented in both material modeling for metal plasticity and process optimization. However, attempts to employ such a technique to phase transformation modeling has not been made. In this work, a sequential improvement algorithm for the identification of dependencies of the model parameters on the experimental conditions of a hot stamping steel 22MnB5 is developed. The algorithm should identify an optimal model for ferrite and bainite while keeping the number of necessary experiments for parameter identification as low as possible.

Materials and Methods

In this section, the concept of implementation of the sequential improvement algorithms on the phase transformation model of ferrite and bainite will be explained. First, the concept of sequential improvement is outlined. Then, material, the approximation of the phase transformation of ferrite and bainite, and modeling of phase transformation and surrogate models to identify the relationship between the process parameters and the independent parameters are explained. Finally, the search algorithms and the termination criteria are presented at the end of the section.

Sequential Improvement Algorithm (SIA). In this work, the sequential improvement algorithm aims to help users to fit appropriate phase transformation models with a minimal number of samples. The work flow of SIA is shown in Fig 1. The algorithm starts by defining the process window for the experiments. Then, the sampling is performed by using Latin hypercube sampling (LHS) where 12 points are sampled in this work, and additional 2^k samples are placed at the edge of the test matrix, where k is a number of dependency parameters. In this case k is equal to 2, i.e., it refers to the cooling rate and pre-strain. In the first iteration, samples containing 1) $\{S_2{}^k\} = 2^2$ additional samples and 2) a first sample chosen by the search algorithms are tested, evaluated and used to construct surrogate models. The loss function measuring the difference between the surrogate model and the experiments are calculated, and checked whether or not the loss meets the termination criteria. If the loss satisfies the termination criteria, the material model is reliable for hot stamping simulation. However, if the loss is bigger than the termination criteria, a new sample is going to be generated by the search algorithm. Finally, the loop is continued until the termination criterion is satisfied or the maximum amount of samples is reached.

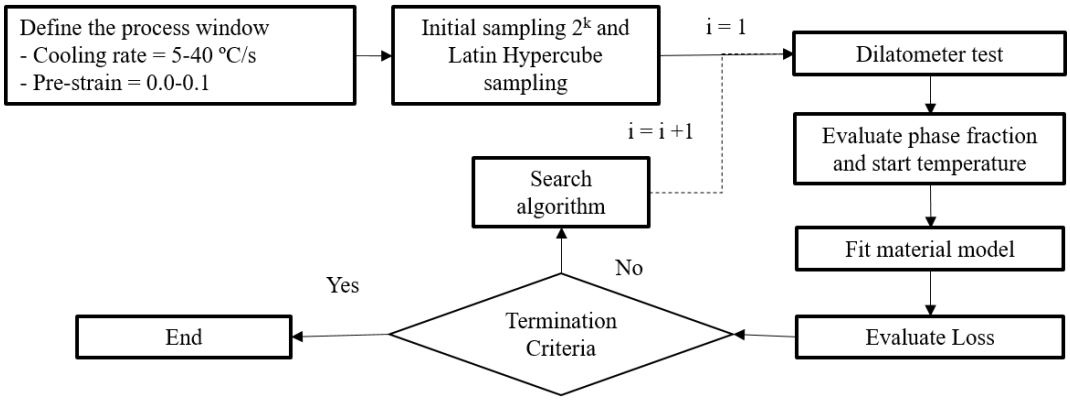

Fig 1 Work flow of the sequential improvement algorithms

Material and dilatometer experiment. A deformation-dilatometer, DIL805 A/D/T, is used to determine phase transformation start temperatures and phase transformation kinetics. A 22MnB5 boron steel with the thickness of 1.5 mm extensively used in hot stamping processes is chosen. The chemical composition of the 22MnB5 is shown in Table 1. The test is performed in vacuum with 10^{-4} mbar and the argon (Ar) is used to quench the specimens. To capture the temperature, the thermocouple type S was spot welded on the specimen surface in the center of the gauge length with the dimensions 5x10 mm. The material is heated to austenitization temperature of 950 °C with a heating rate of 5 K/s. After that, the material is held at this temperature for 300 seconds. The quenching process with the cooling rate of 30 K/s to 800 °C is conducted and the material is deformed. After the deformation the material is quenched down to room temperature with different cooling rates. The experimental set up and the temperature profile used in this experiment are shown in Fig 2 a) and b).

Table 1 Chemical composition of 22MnB5 (Max. wt. %)

Element	C	Mn	Si	Al	Ti	B	Cr	P	S
Max. wt. %	0.22	1.35	0.4	0.08	0.045	0.004	0.25	0.023	0.01

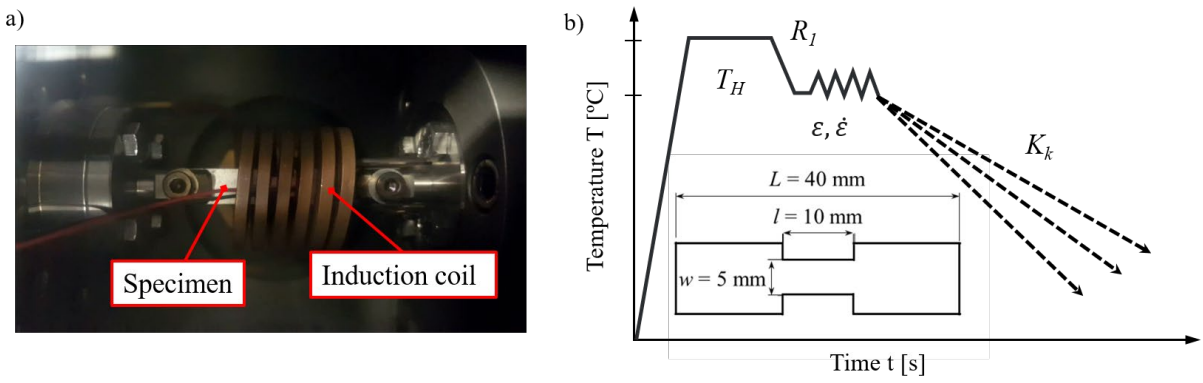

Fig 2 a) Experimental set up and b) temperature profile of the dilatometer experiment

Evaluation of Phase Transformation. To build the material model, the phase transformation kinetics and transformation start temperatures need to be determined. Both can be characterized using lever rule. In the lever rule, the transformed austenite as a function of temperature is calculated by using Eq. 1.

$$X(T) = \frac{l_f}{l_f + l_0} \tag{1}$$

where $X(T)$ is the transformed austenite as a function of temperature and l_0 and l_f are distance between the actual dilatation curve and the start and end lines respectively. To obtain the phase

transformation start temperatures, the transformation start temperature is approximated by using the method in Stahl-Eisen-Prüfblatt SEP 1681 [18].

Modeling of the phase transformation. The accuracy in prediction of the final phase fraction is very important for modeling the hot stamping process. To model a diffusion-controlled phase transformation for the continuous cooling process, the modified Johnson-Mehl-Avrami-Kolmogorov (JMAK) model by Kamamoto et al. [19] is used as shown in Eq. 2.

$$X_i = X_i^{max} - \exp\left(-k\tau(T)^n\right) \text{ with } \tau(T) = \frac{T^s - T}{T^s - T^f} \text{ while } T^s \geq T \geq T^f \quad (2)$$

where X_i is the phase fraction, X_i^{max} is the final volume fraction of ferrite or bainite, k and n are the parameters, T^s and T^f are the phase transforamtion start and finish temperatures, and T is the actual temperature.

Modeling of surrogate model. Surrogate models are employed to establish the relationship between the JMAK parameters and the process parameter. In this study, there are 2 types of surrogate models implemented. The first one is a thin plate spline (TPS) regresseion model as presented by Grzhibovskis et al [20]. TPS is used to fit JMAK parameters (X_i^{max}, k, n), where cooling rate and pre-strain are independent parameters. For the bainite model, where there are three independent parameters (cooling rate, pre-strain, and retain austenite), a polynomial regression is employed when a response variable is non-linear. A second order multiple polynomial regression with 2 independent variables is shown in Eq. 3.

$$y = \beta_0 + \beta_1 x_1 + \beta_2 x_2 + \beta_{11} x_1^2 + \beta_{22} x_2^2 + \beta_{12} x_1 x_2 + \varepsilon \quad (3)$$

where β_1 and β_2 are linear effect parameters, β_{11} and β_{22} are quadratic parameters, and β_{12} is an interaction parameter. In this study, the ferrite and bainite models have different independent parameters. The ferrite model has 2 independent parameters, which are the cooling rate and pre-strain. For the bainite model, the retained austenite is added as another independent parameter.

Search Algorithms. The search algorithms for the SIA is classified into 2 groups. The first group is called exploration. The exploration has the function to fill the design space, while exploitation is used to search a specific area. In the implementation, the exploration is employed at the beginning of the model fitting in order to estimate formed phase fraction in each area, then the exploitation is employed to improve the accuracy of the material model in specifics area.

Exploration search. The exploration starts by dividing the cooling rate into grids where 9x9 grids (grid coordinate system) are set in this case. The start sample is selected from the left hand-side (red dots) at the first grid of the cooling rate, where the first selected sample has a pre-strain close to 0.05 and a cooling rate of 8 K/s. After obtaining the start sample, the next sample is chosen based on the maximum distance d_s between the actual point and the point in the next grid, which can be computed by using Eq. 4.

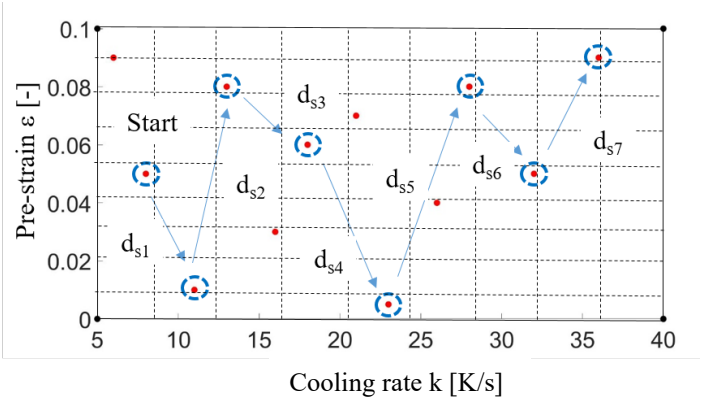

Fig 3 Searching algorithms using exploration

$$d_s = \varphi_{start} - \varphi_{end} \quad (4)$$

where the φ_{start} is pre-strain at the start point , and φ_{end} the pre-stain at the end point. Finally, the exploration is continued until reaching the last grid of the cooling rate as seen in Fig 3.

Exploitation search. The exploitation search will select the next candidate sample based on the maximum error of loss map generated (see Fig. 4 b) from the ferrite and bainite models. At this point,

a set of tested samples consists of $\{S_2^k S\}$, where $\{S_2^k\}$ is additional sample at the edge of the test matrix and {S} is the samples from the exploration. To generate the loss map, the samples are divided into training set $\{S_{train}\}$ and test set $\{S_{test}\}$. The $\{S_{test}\}$ is generated by removing one sample from {S}. The remainder of {S}, from which one sample called $\{S_{train}\}$ has been removed, is used to fit surrogate models of ferrite and bainite. After fitting, the surrogate models are used to predict the value of $\{S_{test}\}$ and the errors between the prediction and experiment are computed, cf. Fig. 4 a). This procedure iterates until all of the samples in S are utilized as $\{S_{test}\}$. After the fitting, the errors between the ferrite and bainite model are added, and the loss map, which represents the amount of error from the ferrite and bainite model, is generated.

To place the next test, the algorithms will search for grids with a maximum error in the loss map and place candidate sample points (white dots in the loss map as seen in Fig *4* b). Then, the distances between each candidate point and its top 3rd nearest neighbour points based on the grid coordinate system are calculated. Following, the expected gain score is computed according to the following Eq. 5.

$$s_i = (d_{i1}w) + (d_{i2}w) + (d_{i3}w) \tag{5}$$

where i is refers to candidate points and s_i is the expected gain score of each candidate point. $d_{i1} - d_{i3}$ are 3rd nearest distances between the candidate and experimental points. The parameter w represents a weight factor that is normalized from the error of experimental points in the loss map. They can be calculated as follows,

$$w_i = \frac{x_i - \min(x)}{\max(x) - \min(x)} \tag{6}$$

where w_i is the i^{th} normalized value in the data set, x_i is the i^{th} value in the data set, $min(x)$ is the minimum value in the data set and $max(x)$ is the maximum value in the data set.

Evaluation of Loss and Termination Criteria. For SIA, the material models are fitted with the sample n. To evaluate the accuracy of models, the model is used to predict the result in the iteration n+1. The error between the calculation and experiment here is called forward error (FE) and can expressed as shown in Ep. 7.

$$FE = \left|Y_{reg\ n+1} - Y_{true\ n+1}\right| \tag{7}$$

where $Y_{reg\ n+1}$ and $Y_{true\ n+1}$ are prediction and experimental results at the iteration *n+1*. Another parameter utilized to track the error along the whole fitting process is called mean absolute error (*MAE*) as express in the following equation Ep. 8.

$$MAE = \frac{1}{n}\sum_{i=1}^{n}\left|Y_{reg} - Y_{true}\right| \tag{8}$$

where Y_{reg} and Y_{true} are prediction and experimental results at the actual iteration. In this study, the termination criterion is reached when the deviation between FE and MAE for both ferrite and bainite model are less than equal to 0.05, which can be set individually.

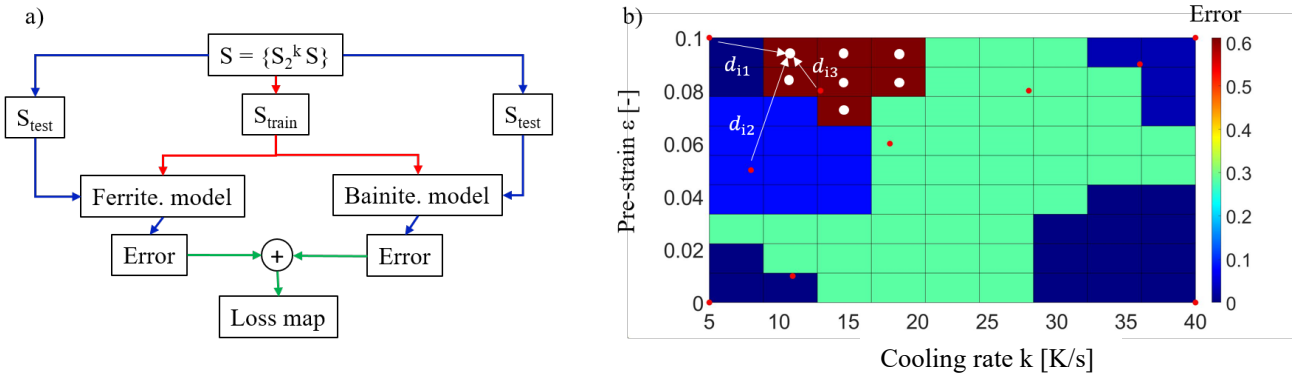

Fig 4 a) Procedure to construct loss map and b) the loss map

Results and Discussion

The result from the execution of SIA is presented in this section. First, the fitting of the JMAK model from the kinetics of the phase transformation calculated by using the lever rule is shown. Then, the results of the SIA are presented. Finally, the ferrite and bainite models obtained from the SIA are validated using 3 additional, independent samples that were not used for parameter fitting.

Fitting of the material model. From the dilatometer experiments, the dilatation data as shown in Fig 5 a) is obtained. By using the lever rule, the dilatation can be transformed into the phase transformation kinetics. Finally, the kinetics are used to fit JMAK-type models. Fig 5 b) shows an example of the comparison between the JMAK models and the experimental results.

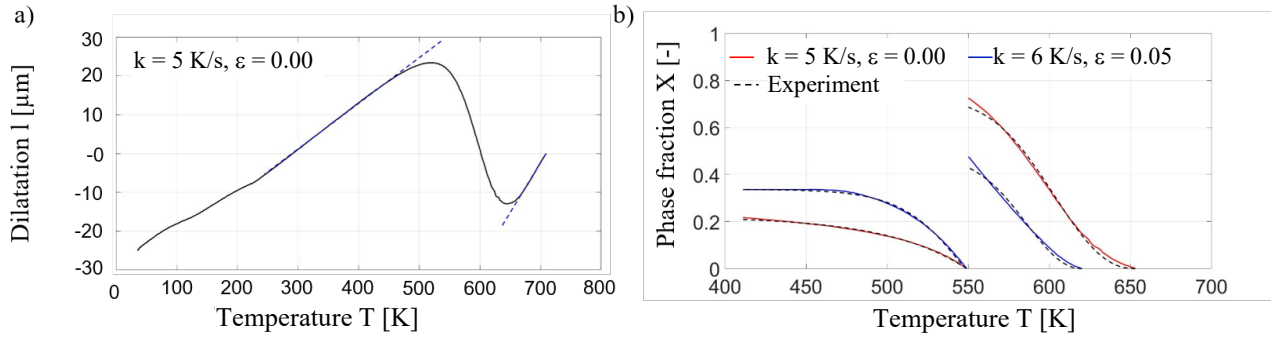

Fig 5 a) Experimental result from the cooling rate of 5 K/s with pre-strain of 0.00 and b) comparison between JMAK and experimental results

Results of SIA. SIA applied 2 searching algorithms to search for the next candidate sample. The exploration is applied at the iterations 1-6. After the iteration 6, the exploitation algorithm is executed. Fig 6 a) shows the evolution of errors of the ferrite model. The results show that after iteration no. 3 the errors of the ferrite model are constant because at the samples 4-6, there no ferrite is formed. After the exploitation, the ferrite model meets the termination criterion at iteration no. 8. For the bainite model, the errors calculated from the model gradually decrease during the exploration. After implementing the exploitation algorithms, the bainite model satisfies the termination criterion and the error is stable because the bainite model is already fitted well with the experimental results as shown in Fig 6 b).

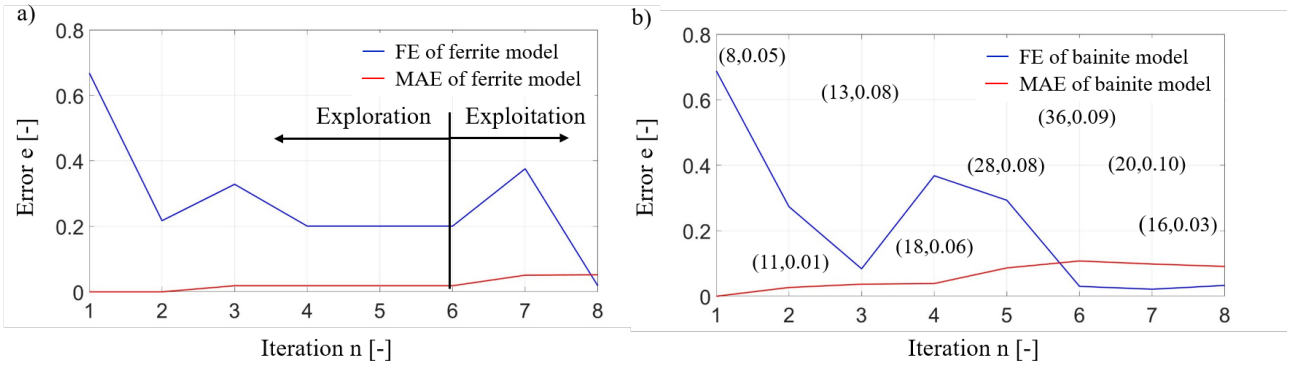

Fig 6 Mean absolute error (MAE) and forward error (FE) from the exploration algorithms of a) the ferrite model and b) the bainite model

Validation of SIA. To evaluate the effectiveness of the SIA, material models generated from the SIA are validated with 3 additional samples. The results of the validation are presented in Fig 7. The models created by using SIA predict the experimental data well. However, at the cooling rates of 16 K/s and 20 K/s, there is small amount of ferrite measured during the experiments where there is no ferrite calculated by SIA. Although the models created using SIA cannot fully capture phase transformation, the prediction of phase transformation is acceptable.

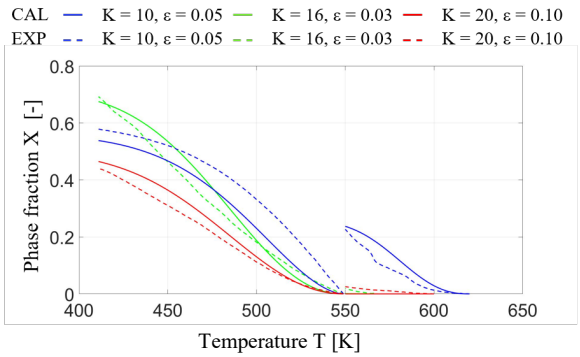

Fig 7 Validation of SIA model

In this work, the sequential improvement algorithm is utilized to fit phase the transformation models at reduced experimental cost compared to the DOE methods presented in the introduction. The proposed method provides some advantages. Assuming that full-factorial design is performed with 2 factors on 3 levels, the cooling rates are 5, 20, and 40 K/s and the pre-strains are 0, 0.05, and 0.1. If the model is fitted according to this condition, the phase transformation model will have less information for the cooling rate, and the accuracy of the models will drastically decrease. A half-factorial design is not appropriate for 2 factors. With conventional DOE all experiments have to be performed before fitting of the models. As a result, some experiments gain only little additional information for parameter identification, for example at the high cooling rates of 30-40 ºC/s, which is above the critical cooling rate. With the SIA, only 4 experiments are placed in this range and most of the samples are between the cooling rate of 5-25 K/s. The selection of the next sampling point is calculated based on the accuracy of the ferrite and bainite models, which is impossible for the conventional DOE. Compared to the DOE, the SIA offers advantages in fitting phase transformation models.

Conclusion

Sequential improvement algorithms for identification of the phase transformation model of ferrite and bainite was presented. The following conclusions can be drawn: 1) The SIA allows automatic selection of testing conditions. 2) The search for the next experimental test condition should be done through exploration and exploitation. 3) The accuracy of the predicted model under unknown test conditions can be estimated efficiently by thin plate spline for ferrite model and multivariable polynomial regression for the bainite model. 4) The new test condition is found by using expected gain score. Using this method, the global and local effects of phase changes can be explored and the number of experiments for modeling the hot stamping steel 22MnB5 under continuous cooling can be drastically reduced to 12 instead of 30-40 samples.

Acknowledgements

The results presented were achieved in the projects “Intelligente Prüfmaschine” and “Virtuelles Dilatometer”. The research project IFG 20071 BG / P 1305/18/2019 "Virtuelles Dilatometer" from the Research Association for steel Application (FOSTA), Düsseldorf and the “Intelligente Prüfmaschine” (IFG 20637BG) by the European Research Association for Sheet Metal Working (EFB) was supported by the Federal Ministry of Economic Affairs and Climate Action through the German Federation of Industrial Research Associations (AiF) as part of the programme for promoting industrial cooperative research (IGF) on the basis of a decision by the German Bundestag. The project Intelligente Prüfmaschine was carried out at the Chair of Hybrid Manufacturing, Brandenburg University of Technology in Cooperation with the Institute of Manufacturing Technology, Friedrich-Alexander-Universität Erlangen-Nürnberg and respectively project “Virtuelles Dilatometer” with the Fraunhofer-Institut für Werkstoffmechanik IWM, Freiburg.

References

[1] Karbasian H, Tekkaya AE. A review on hot stamping. *Journal of Materials Processing Technology* 2010;210:2103–18, doi:10.1016/j.jmatprotec.2010.07.019.

[2] Merklein M, Wieland M, Lechner M, Bruschi S, Ghiotti A. Hot stamping of boron steel sheets with tailored properties: A review. *Journal of Materials Processing Technology* 2016;228:11–24, doi:10.1016/j.jmatprotec.2015.09.023.

[3] Åkerström P, Bergman G, Oldenburg M. Numerical implementation of a constitutive model for simulation of hot stamping. *Modelling Simul. Mater. Sci. Eng.* 2007;15:105–19, doi:10.1088/0965-0393/15/2/007.

[4] Hippchen P, Lipp A, Grass H, Craighero P, Fleischer M, Merklein M. Modelling kinetics of phase transformation for the indirect hot stamping process to focus on car body parts with tailored properties. *Journal of Materials Processing Technology* 2016;228:59–67, doi:10.1016/j.jmatprotec.2015.01.003.

[5] Aziz N, Aqida SN. Hot Press Forming of 22MnB5 Steel Using Full Factorial Design of Experiment (DOE). *AMR* 2014;1024:243–6, doi:10.4028/www.scientific.net/AMR.1024.243.

[6] You KH, Kim H-K. A Study on the Effect of Process and Material Variables on the Hot Stamping Formability of Automotive Body Parts. *Metals* 2021;11:1029, doi:10.3390/met11071029.

[7] Horn A, Merklein M. Functional optimization of hot-stamped components by local carburization. *International Journal of Lightweight Materials and Manufacture* 2020;3:43–54, doi:10.1016/j.ijlmm.2019.09.002.

[8] Paul D. BergerRobert E. MaurerGiovana B. Celli. *Introduction to Taguchi Methods*: Springer; 2018.

[9] Richard F. Gunst, Robert L. Mason. Fractional factorial design. *WIREs Computational Statistics* 2009; 1.

[10] Wong WH, Lee WX, Ramanan RN, Tee LH, Kong KW, Galanakis CM, Sun J, Prasad KN. Two level half factorial design for the extraction of phenolics, flavonoids and antioxidants recovery from palm kernel by-product. *Industrial Crops and Products* 2015;63:238–48, doi:10.1016/j.indcrop.2014.09.049.

[11] Anthony Atkinson, Alexander Donev, Randall Tobias. *Optimum Experimental Designs, With SAS*: OUP Oxford; 2007.

[12] Pukelsheim F. *Optimal design of experiments*: Philadelphia, PA: Society for Industrial and Applied Mathematics (SIAM); 2006.

[13] Lohmar J, Bambach M, Hirt G, Kiefer T, Kotliba D. The Precise Prediction of Rolling Forces in Heavy Plate Rolling Based on Inverse Modeling Techniques. *steel research int.* 2014;85:1525–32, doi:10.1002/srin.201300431.

[14] Vladimirov IN, Bambach M, Herty M, Bücker HM. Identification of optimal material models and parameters in finite strain plasticity. *Proc. Appl. Math. Mech.* 2013;13:335–6, doi:10.1002/pamm.201310163.

[15] Bambach M, Bücker HM, Heppner S, Herty M, Vladimirov IN. Characteristics of testing conditions for constitutive models in metal plasticity. *J Eng Math* 2014;88:99–119, doi:10.1007/s10665-013-9681-2.

[16] Bambach, M., Imran, M., Buhl, J., Härtel, S., Awiszus, B. Towards intelligent mate-rials testing with reduced experimental effort for hot forming. *Computer Methods in Materials Science* 2017.

[17] Wiebenga JH, van den Boogaard AH, Klaseboer G. Sequential robust optimization of a V-bending process using numerical simulations. *Struct Multidisc Optim* 2012;46:137–53, doi:10.1007/s00158-012-0761-0.

[18] Verein Deutscher Eisenhüttenleute. SEP 1681: Richtlinien für Vorbereitung, Durchführung und Auswertung dilatometrischer Umwandlungsuntersuchungen an Eisenlegierungen, Stahleisen, 1998

[19] Kamamoto S, Nishimori T, Kinoshita S. Analysis of residual stress and distortion resulting from quenching in large low-alloy steel shafts. *Materials Science and Technology* 2013;1:798–804, doi:10.1179/mst.1985.1.10.798.

[20] Grzhibovskis R, Bambach M, Rjasanow S, Hirt G. Adaptive cross-approximation for surface reconstruction using radial basis functions. *J Eng Math* 2008;62:149–60, doi:10.1007/s10665-007-9197-8.